

RESEARCH PAPER

Enhancement of Non-Linear Optical laser Power-Depend Properties of ZnO Nanoparticle Synthesized by Green Method

Samir M. Hamad ¹, Akram Rostaminia ², Eman A. Saied ³, Mahira M. Esmael ³, Azeez Barzinjy ^{1,4}, Peyman Aspoukeh ^{1*}, Hossein Khojasteh ¹

¹ Scientific Research Center, Soran University, Kurdistan Region, Iraq

² Department of Medical Biochemical Analysis, Cihan University-Erbil, Kurdistan Region, Iraq

³ Department of Physics, College of Science, Salahaddin University-Erbil, Kurdistan Region, Iraq

⁴ Physics Education Department, Faculty of Education, Tishk International University, Kurdistan Region, Iraq

ARTICLE INFO

Article History:

Received 16 April 2025

Accepted 19 August 2025

Published 01 October 2025

Keywords:

Green synthesis

Optical properties

Structural properties

Z-Scan

ZnO NPs

ABSTRACT

This study explores the green synthesis of zinc oxide nanoparticles (ZnO NPs) using mint plant extracts, emphasizing their applicability in photonic technologies. Verified by Scanning Electron Microscopy (SEM), the nanoparticles, approximately 80 nm in size, exhibited enhanced nonlinear optical properties suitable for optical limiting applications. Employing open and closed aperture Z-scan techniques at wavelengths of 532 nm and 635 nm, the nanoparticles demonstrated nonlinear absorption coefficients ranging from 0.5 cm/GW to 187 cm/GW and refractive indices between 2.51×10^{-13} and 5.81×10^{-13} cm²/W, underscoring their potential for advanced optical applications. The involvement of plant-derived functional groups, confirmed by Fourier Transform Infrared Spectroscopy (FTIR) and Energy-dispersive X-ray Spectroscopy (EDX), was critical in acting as reducing, capping, and stabilizing agents. These agents contributed significantly to the structural and compositional integrity of the ZnO nanoparticles. The study highlights the effectiveness of using plant-based synthesis methods, not only in enhancing the nanoparticles' optical properties but also in promoting sustainable material development in the field of photonics.

How to cite this article

Hamad S., Rostaminia A., Saied A. et al. Enhancement of Non-Linear Optical laser Power-Depend Properties of ZnO Nanoparticle Synthesized by Green Method. J Nanostruct, 2025; 15(4):1753-1765. DOI: 10.22052/JNS.2025.04.024

INTRODUCTION

The field of nonlinear optical (NLO) materials has garnered significant attention due to advancements in powerful ultrafast lasers [1]. These materials are integral to a variety of applications, including optical limiting, optical computing, and optical communication [2], as well as nonlinear optical spectroscopy [3, 4] and biomedical fields [5]. As we look to the future, the expected capabilities of optoelectronic

devices include outstanding performance, high operational speeds, and compact designs. Among the diverse materials employed in these technologies, metal/metal oxide nanoparticles and nanocomposites are particularly notable. Celebrated for their unique surface effects and quantum confinement properties, which are absent in their bulk counterparts, these materials enhance the functionality of optical devices [6].

Among these innovative materials, Transparent

* Corresponding Author Email: peyman.aspoukeh@soran.edu.iq



Conducting Oxide (TCO) nanomaterials stand out due to their exceptional optical and electrical properties. These materials, which include wide bandgap semiconductors like zinc oxide (ZnO), are essential in many optoelectronic devices. They combine semiconductor properties with a transparency that is crucial for applications requiring the manipulation of visible light and sufficient carrier density to ensure electrical conductivity [7, 8]. Zinc oxide nanoparticles, in particular, are renowned not only for their applications in fields such as UV light emitters and piezoelectric transducers but also for their biocompatibility, making them suitable for biomedical applications [9].

The synthesis of ZnO nanoparticles through physical [10], chemical [11], and, biological methods [12], presents varied environmental and economic challenges. Physical methods often demand high pressures and temperatures, making them costly and environmentally burdensome [13]. Chemical methods, while effective, pose significant environmental and safety risks due to hazardous chemicals used as reducing agents [14]. Conversely, biological synthesis using natural agents such as plant extracts, fungi, and bacteria provides a greener, safer alternative [15, 16]. This study explores the innovative synthesis of ZnO nanoparticles using mint plant extracts, a method that not only supports sustainable material development but also potentially enhances the nanoparticles' optical properties due to the unique interactions of plant-derived phytochemicals.

Beyond their sustainable synthesis, ZnO nanoparticles exhibit exceptional physical properties that justify their widespread use in advanced applications [17]. Recent studies have highlighted their capabilities in high-speed carrier dynamics and significant nonlinear refraction and absorption, crucial for the development of broadband optical networks where high-speed optical switching devices are essential [18, 19]. These devices require materials with minimal optical losses and rapid response times, achievable through materials like ZnO with a band gap at least twice the photon energy employed [20-22].

The Z-scan technique, extensively used to assess the intensity-dependent nonlinear susceptibilities of materials, including their nonlinear refractive index and absorption characteristics, plays a pivotal role in our study [23, 24]. This highly sensitive method, developed by Sheik-Bahae et

al. [23], is crucial for measuring how materials respond to varying light intensities, a critical factor in the development of optical limiting devices that operate based on nonlinear absorption or refraction.

In this study, we synthesize zinc oxide (ZnO) nanoparticles using a novel green synthesis method with mint plant extracts, analyzing their nonlinear optical properties through both closed and open aperture Z-Scan techniques at varying laser powers and wavelengths. This approach not only highlights the sustainability of using phytochemicals in nanoparticle fabrication but also suggests that these compounds enhance the nonlinear refractive index and absorption characteristics of ZnO NPs. Our findings underscore the potential of integrating environmentally sustainable methods with advanced optical applications, paving the way for high-performance materials that leverage biological synthesis to optimize material properties uniquely. This synthesis method aligns with environmental goals and opens new avenues for material functionality that traditional methods cannot achieve, making it a significant contribution to the field of material science.

MATERIALS AND METHODS

Chemicals and Materials

In this study, double-distilled water was used for both the growth and treatment processes. All chemical materials, such as zinc nitrate hexahydrate ($\text{Zn}(\text{NO}_3)_2 \cdot 6\text{H}_2\text{O}$) and sodium hydroxide (NaOH), were sourced from Sigma-Aldrich and used as received, without undergoing additional purification. This standardization of reagents ensures reliability and consistency in the experimental setup, facilitating reproducible results across various research trials.

Plant collection

Fresh and healthy mint leaves were collected from Rawanduz city, located at coordinates 36.1901° N, 43.9930° E, in the Erbil Governorate of the Kurdistan Region, Iraq. This specific sourcing of mint leaves ensures the consistency and ecological relevance of the plant materials used in the study.

ZnO Green Synthesize

Twenty-five grams of fresh, seasonal mint leaves were harvested, washed, chopped into small pieces, and then boiled in 200 mL of double-

distilled water at 70 °C for 40 minutes. The resulting aqueous extract was filtered using Whatman No.1 filter paper and refrigerated for later use. For the synthesis of zinc oxide nanoparticles (ZnO NPs), 50 mL of the mint leaf extract was gradually mixed with an equal volume of zinc nitrate [$\text{Zn}(\text{NO}_3)_2$] solution while being continuously stirred magnetically at 80 °C for 45 minutes. The pH of the mixture was adjusted by adding 1 M sodium hydroxide (NaOH) until a color change occurred, indicating the start

of ZnO NP nucleation. This color shift, which can be monitored by UV/Vis double beam spectroscopy, is typically accompanied by the formation of white sediment and signifies nanoparticle formation, with a yellowish hue indicating the presence of ZnO NPs. Following this, the sediment was separated by centrifugation at 7000 rpm for 30 minutes. The collected solid powder was then rigorously washed with methanol and distilled water four times to remove any impurities and

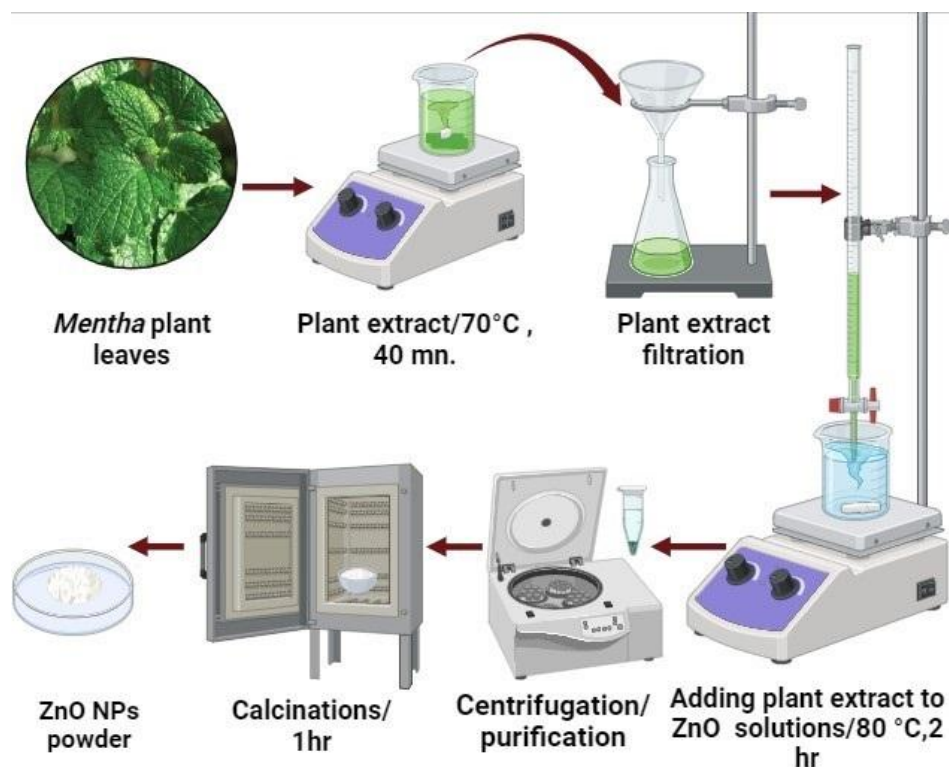


Fig. 1. Schematic diagram of green synthesized ZnO nanoparticles.

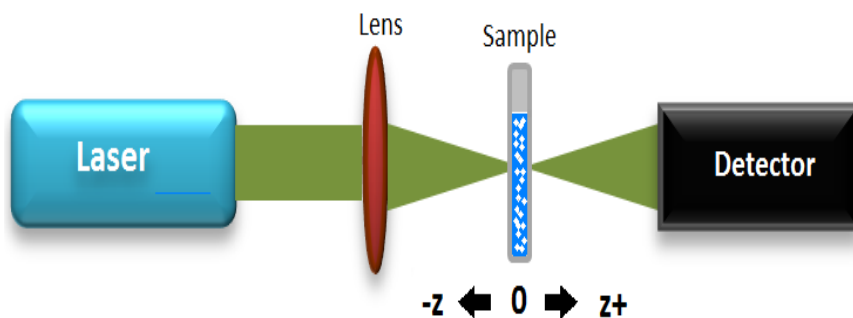


Fig. 2. Z-Scan experiment setup.

organic residues. Finally, the sample was partially annealed on a Bunsen burner at 500°C for 1 hour to enhance its properties, as shown in Fig. 1. This method effectively demonstrates the production of nanomaterials, providing visual and spectroscopic evidence of the synthesis process.

Z-Scan System

Fig. 2 illustrates the setup for the Z-Scan technique. To synthesize the ZnO nanoparticles (NPs), ZnO nanomaterial was dispersed in 70 milliliters of distilled water. This mixture was prepared in different concentrations, labeled as samples C1, C2, and C3. The mixtures were then stirred on a magnetic stirrer for 30 minutes to ensure a homogeneous white solution was achieved. This setup is critical for examining the nonlinear optical properties of the ZnO nanoparticles under varying conditions.

Therefore, volume fraction (V) was computed using the Eq. 1;

$$V = \frac{V_s}{V_s + V_L} \quad (1)$$

Where V_L is the liquid volume, $V_s = m/\rho$ is the volume of ZnO NPs, ρ is the ZnO density, and m is the mass of ZnO particle dispersed in solution, the detail of results is listed in the (Table 1).

Green and red Z-Scan measurements were utilized to examine the nonlinear optical (NLO) response of each sample, employing different laser powers to demonstrate the impact of laser power on NLO characteristics. The results of these measurements are detailed in (Table 2). This approach allows for a comprehensive analysis of how varying laser power levels affect the NLO properties of the samples, providing valuable

insights into their potential applications in optical devices.

Characterization techniques

X-ray diffraction measurements were performed using a PANalytical X' Pert PRO instrument equipped with CuK α radiation ($\lambda = 1.5406 \text{ \AA}$). The scans were conducted at a rate of 1° per minute across a 2θ range of 20° to 80°. The synthesis and presence of ZnO nanoparticles were verified using a UV-Vis double-beam spectrophotometer (Super Aquarius-1000). Additionally, the morphology of the nanoparticles was examined using ionic emission scanning electron microscopy (SEM-Quanta 450). To determine the chemical composition of the synthesized nanostructures, energy-dispersive X-ray spectroscopy (EDS) analyses were performed within the SEM setup. FTIR spectroscopy was conducted using a Perkin Elmer spectrometer with a resolution of 4 cm⁻¹ to investigate the functional groups present in the synthesized ZnO NPs. This comprehensive set of analytical techniques ensures a thorough characterization of the ZnO nanoparticles, confirming their structure, composition, and physical properties.

RESULTS AND DISCUSSION

ZnO Nanoparticles Characterization

UV-Vis Analysis

The optical properties of zinc oxide nanoparticles (ZnO NPs) were investigated using ultraviolet-visible (UV-Vis) absorption spectroscopy. This technique is pivotal for confirming the successful synthesis of ZnO NPs, as the oscillations of conducting electrons within specific wavelength ranges provide insight into the surface plasmon

Table 1. ZnO NPs concentration's and volume fraction for different samples.

Samples	ZnO NPs in 70 ml DDW/g	$V_s \times 10^{-4} / \text{m}^3$	$V_L \times 10^{-5} / \text{m}^3$	$V \times 10^{-4} / \text{m}^3$
C ₁	0.0158	6.6	7	0.9999883
C ₂	0.0260	10.97	7	0.9999936
C ₃	0.0301	12.7	7	0.9999944

Table 2. laser characteristics used in Z-Scan.

Lasers	Wavelength /nm	Power /mW
1	532	100
2	532	1000
3	532	10000
4	635	200

resonance (SPR) effect. As shown in Fig. 3, the UV-Vis spectrum of the synthesized ZnO NPs features an absorption band centered at 365 nm, which confirms their presence in the solution. Notably, the absence of any additional absorption peaks in the spectrum indicates the purity of the ZnO NPs, free from other elemental or biomolecular impurities. These findings are consistent with results from previous studies [18-20], reinforcing the reliability of the synthesis and characterization methods used.

X-Ray Diffraction Analysis for ZnO NPs

The X-ray diffraction (XRD) patterns of ZnO nanoparticles (NPs) synthesized through green methods are depicted in Fig. 4. The identified peaks at 31.90°, 34.57°, 36.41°, 47.70°, 56.76°, 62.97°, 66.58°, 68.07°, 69.21°, 72.75°, 76.98°, and 81.51° correspond to the lattice planes (100), (002), (101), (012), (110), (013), (200), (112), (201), (004), and (202) respectively. These planes are consistent with the hexagonal wurtzite structure of ZnO, as indexed by the Joint Committee on Powder Diffraction Standards (JCPDS-36-1451). The absence of additional peaks and signals confirms the phase purity of the ZnO NPs. At room temperature, the lattice constants of the ZnO sample were determined to be 3.2346 Å for the 'a' parameter and 5.2120 Å for the 'c' parameter. The presence of narrow and intense diffraction peaks, particularly for the (100), (002), and (101) planes, underscores the high crystalline quality of the ZnO

sample. Using the Debye-Scherrer formula, the estimated size of the ZnO NPs was calculated from the XRD data:

$$D = \frac{0.94}{\beta \cos \theta} \quad (2)$$

Where D is the crystalline size, λ is the X-ray wavelength, equals to 1.5406 Å, and β is the full width half maximum (FWHM) of the dominant peak (101), ~0.003. Therefore, the average crystalline size of the ZnO NPs can be calculated to be in the range of 70–80 nm. The obtained XRD result of ZnO NPs is in good agreement with previous work [25, 26].

SEM and EDS Analysis

SEM analysis of ZnO nanoparticles, synthesized using a green method with mint plant extracts, reveals a morphology characterized by predominantly spherical nanoparticles that tend to cluster into aggregates. This aggregation, observable in the SEM images, is typical of nanoparticles synthesized through environmentally friendly methods, where natural compounds act as stabilizing agents. The detailed SEM image provides insight into the anisotropic nature of these nanoparticles and their surface characteristics at the nanoscale level.

Complementing the SEM analysis, the particle size distribution histogram (Fig. 5) provides a quantitative insight into the size range of the

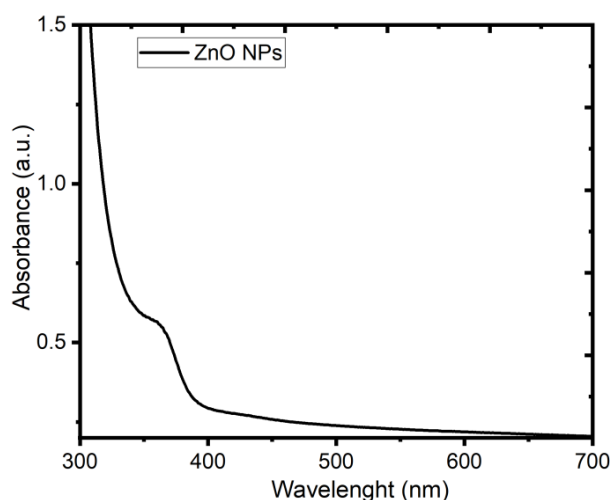


Fig. 3. UV-Vis Spectrum of green synthesis of ZnO nanoparticles.

synthesized nanoparticles. The peak of the distribution curve occurs at approximately 80 nm, indicating a modal particle size that is optimal for the intended applications in photonic devices. The controlled particle size distribution not only reflects the efficacy of the green synthesis method but also suggests that the size and uniformity of these nanoparticles are conducive to enhancing their nonlinear optical properties. The precise control of particle size is crucial for applications that rely on the specific interaction of light with matter, such as in optical limiting and high-speed

optical switching devices, where the nanoparticles' ability to respond to light at ultrafast speeds is essential.

To gain deeper insights into the topographical features of ZnO nanoparticles (NPs), Energy-dispersive X-ray (EDS) analysis was conducted on the same region scanned by the SEM, as shown in Fig. 6. The elemental analysis revealed that the ZnO NPs consist of approximately 78.5% zinc (Zn) and 21.5% oxygen (O), demonstrating high levels of purification [27]. Zn and O are the primary components of the ZnO sample and are uniformly

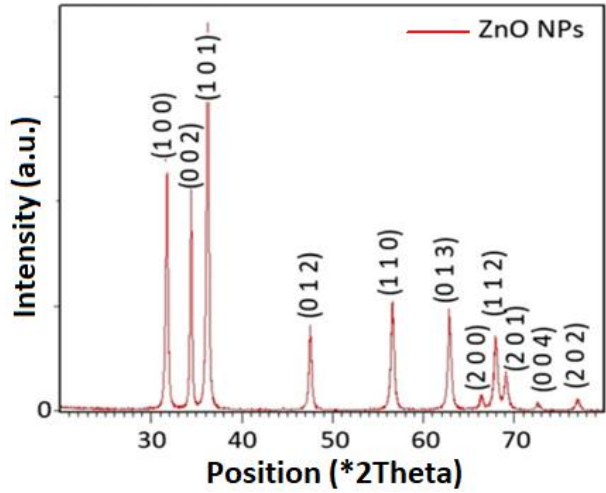


Fig. 4. XRD patterns of green synthesis ZnO nanoparticles.

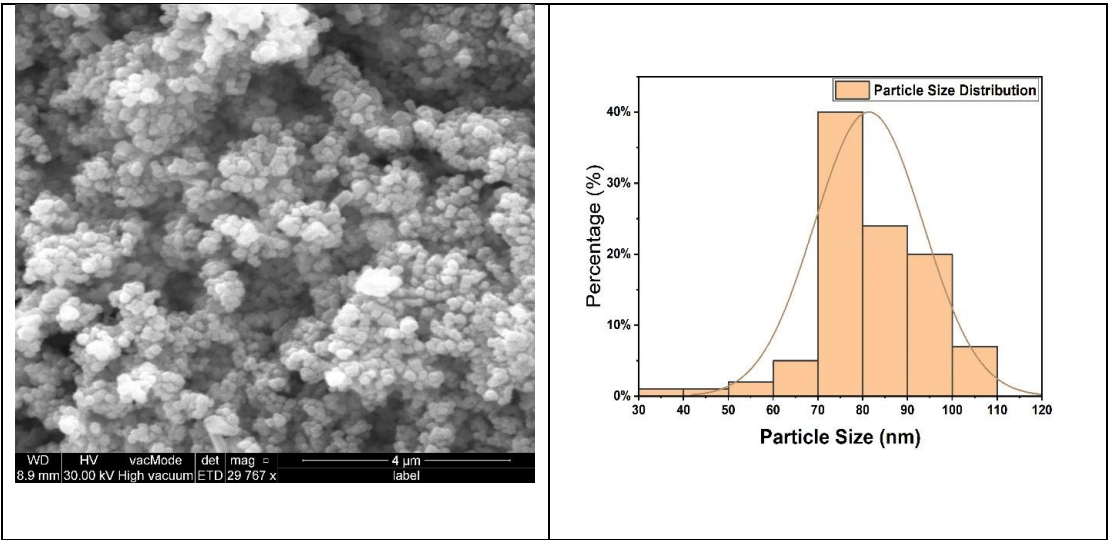


Fig. 5. SEM image and particle size distribution histogram of green synthesized ZnO nanoparticles.

dispersed across the surface of the nanoparticles. The presence of gold (Au) detected in the EDS analysis is attributed to the gold coating applied to the samples to enhance the quality of SEM imaging. The combined results from the X-ray diffraction peaks, SEM images, and EDS analysis confirm that the synthesized ZnO NPs are of high quality, free from impurities or secondary phases.

FTIR Analysis

Fourier-transform infrared (FT-IR) spectroscopy was utilized to confirm the purity and characteristics of the green-synthesized ZnO nanoparticles (NPs). Metal oxides, including ZnO, often show absorption bands in the fingerprint region below 1000 cm^{-1} , which are indicative of interatomic vibrations. The FT-IR spectrophotometer was thus employed to assess the composition and structural integrity of the ZnO NPs. Additionally, the FT-IR spectrum offers insights into the types of bonding present within the samples across all phases of matter [28].

The FT-IR spectra for the powdered samples of synthesized ZnO NPs, as displayed in Fig. 7, reveal several key features. The broad absorption peak at approximately 3323 cm^{-1} is attributed to the O–H stretching vibrations of intermolecular

hydrogen bonds, possibly due to atmospheric moisture absorption. The peak around 1467 cm^{-1} is linked to the amine (N–H) groups from proteins or enzymes present in the plant extract used in the synthesis. Another peak at 1062 cm^{-1} corresponds to the C–O bond, indicative of carbohydrate presence. The peak at 878.31 cm^{-1} likely stems from polyphenolic groups in the plant extract, which act as capping agents [29]. Finally, the sharp peak observed around 402 cm^{-1} is attributed to the Zn–O stretching vibrations specific to the ZnO NPs, confirming their presence and purity. These findings are consistent with previous research [30–32], demonstrating the successful synthesis of high-quality ZnO nanoparticles using green methods.

Mechanism of Green Synthesis ZnO Nanoparticles

Plant extracts are rich in a diverse array of compounds, including flavonoids, terpenoids, and polyphenols, which facilitate the bio-reduction of metal salt solutions during nanoparticle synthesis. These natural substances serve as reduction, capping, and stabilization agents—roles that are crucial in the synthesis of nanoparticles. Traditionally, chemical agents have been used for these purposes; however,

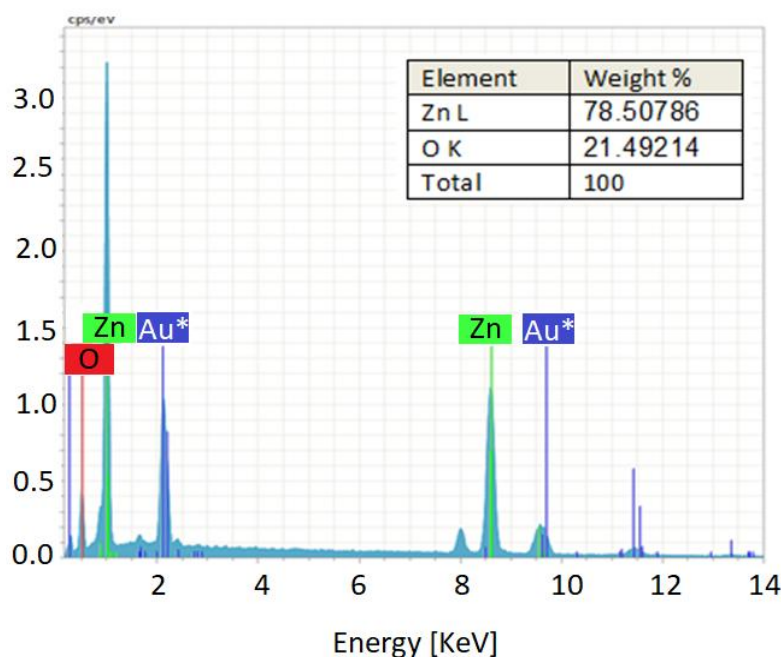


Fig. 6. EDS analysis of ZnO nanoparticles.

they pose significant environmental and health risks due to their potential for degradation and toxicity. Consequently, there is a pressing need for environmentally friendly alternatives that can fulfill these roles in nanostructure preparation.

Phytochemicals present in various parts of plants—such as stems, fruits, roots, peels, seeds, flowers, and leaves—offer a promising alternative to chemical agents. These phytochemicals are believed to be responsible for the reduction of metal ions to zero-valent metal nanoparticles [33]. This reduction process is often indicated by color changes in the reaction solution, which can be monitored using UV-Vis spectroscopy [34]. Research has shown that mint extract, in particular, contains flavonoids and phenolic acids that significantly aid in the reduction of zinc ions

and stabilize the growth of ZnO nanoparticles [35].

Illustrated in Fig. 8, the mechanism of nanoparticle growth highlights the potential biomolecules in the plant extract responsible for bio-reducing metal ions, initiating nucleation, and subsequently promoting the growth of ZnO nanoparticles in various sizes and shapes. According to this mechanism, and given the presence of hydroxyl (OH) groups in phytochemicals, zinc ions (Zn^{2+}) undergo reduction to zero-valent zinc (Zn^0). During the annealing process, due to high oxidation potential of Zn^0 , it readily reacts with oxygen, leading to the spontaneous formation of ZnO nanoparticles [36]. This synthesis approach not only reduces environmental impact but also enhances the biocompatibility of the nanoparticles, making them suitable for various

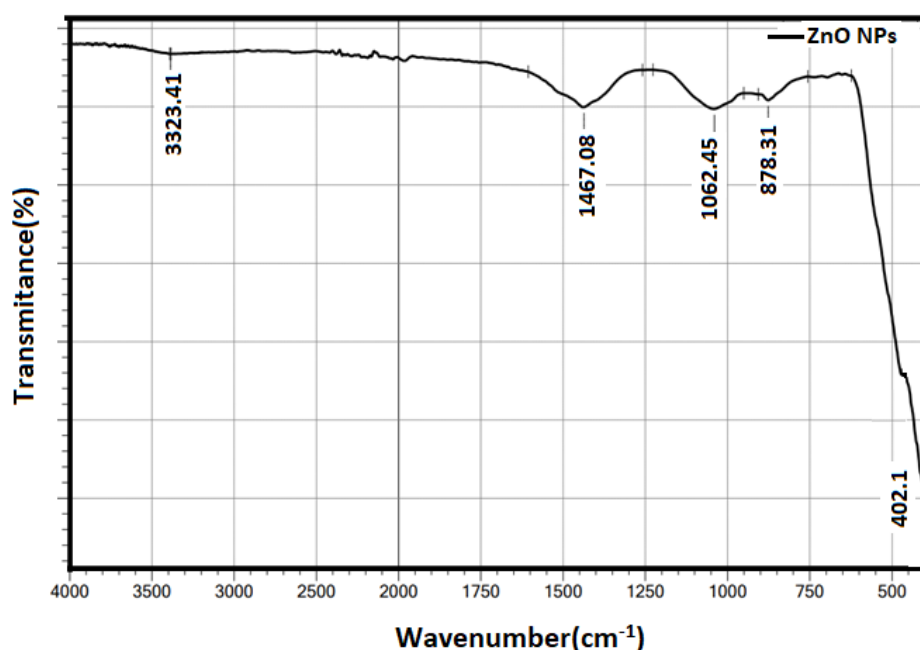


Fig. 7. FT-IR Spectrum of green synthesis ZnO NPs.

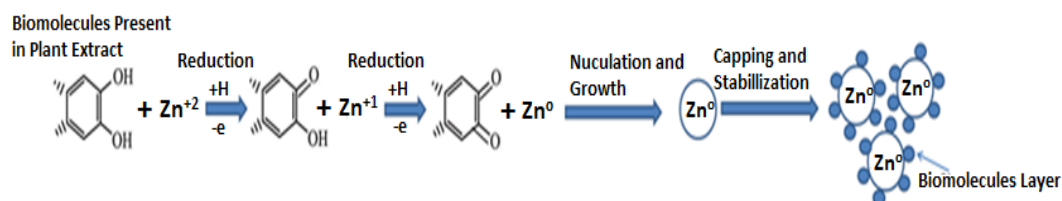


Fig. 8. reducing and capping ability of parsley leaf extracts to produce ZnO NPs.

applications.

Non-Linear Optical Properties

Fig. 1 depicts the experimental setup for the Z-scan experiment, modeled after the setup used in the work of Zhang et al. [37]. It should be noted that the experiment was conducted at room temperature utilizing continuous wave (CW) green and red laser diodes, operating at wavelengths of 532 nm and 635 nm, respectively. A 10 cm focal length convex lens was employed to focus the laser beam to a small spot, and a micro-stepping controller was used to precisely adjust the sample's position along the Z-axis. The nonlinear refractive index was measured by moving a glass optical cell ($L=2$ cm), containing the sample solution, through the beam's focus along the Z-axis. The nonlinear absorption (NLA) coefficient was then determined based on the Z-scan experiments conducted using both closed aperture (CA) and open aperture (OA) settings.

Measurements on ZnO nanocolloids were performed using the Z-scan technique on three different concentrations of ZnO NPs, irradiated at excitation wavelengths of 532 nm and 635 nm with varying incident peak intensities ranging from 110.14 MW/cm² to 31831 MW/cm² for the 532 nm wavelength and 248.67 MW/cm² for the 635 nm wavelength. The OA Z-scan traces of the ZnO NPs colloids, illustrated in Fig. 9 (a-d), consistently show a valley, aligning with previous findings [38]. This characteristic can be attributed to reverse saturable absorption (RSA) behavior, likely caused

by the absorption of free carriers and excitation effects [39]. The nonlinear absorption coefficient was calculated using the Eq. 3:

$$\beta = \frac{2\sqrt{2}\Delta T}{I_0 L_{\text{eff}}} \quad (3)$$

Where ΔT is the single valley value at the Z-scan curve's, I_0 intensity of laser and L_{eff} is effective sample length given by;

$$L_{\text{eff}} = \frac{1 - e^{-\alpha_0 L}}{\alpha_0} \quad (4)$$

Where, α_0 is linear absorption, and L is sample length.

In the open aperture scan results, as detailed in (Table 3), there is a clear increase in the nonlinear absorption coefficient as the concentration of nanoparticles in the solution increases. Specifically, when the concentration of ZnO NPs colloids is increased from C1 to C2 g/70mL, a greater number of nanoparticles are present, which enhances the occurrence of three-photon absorption (3PA). The obtained 3PA coefficient from these measurements is three times larger than that observed in thin films and eight times larger than in bulk zinc. These results align with those reported in previous studies [40], confirming the enhanced nonlinear optical properties of ZnO NPs in colloidal form compared to more traditional physical states.

The nonlinear absorption coefficient, observed

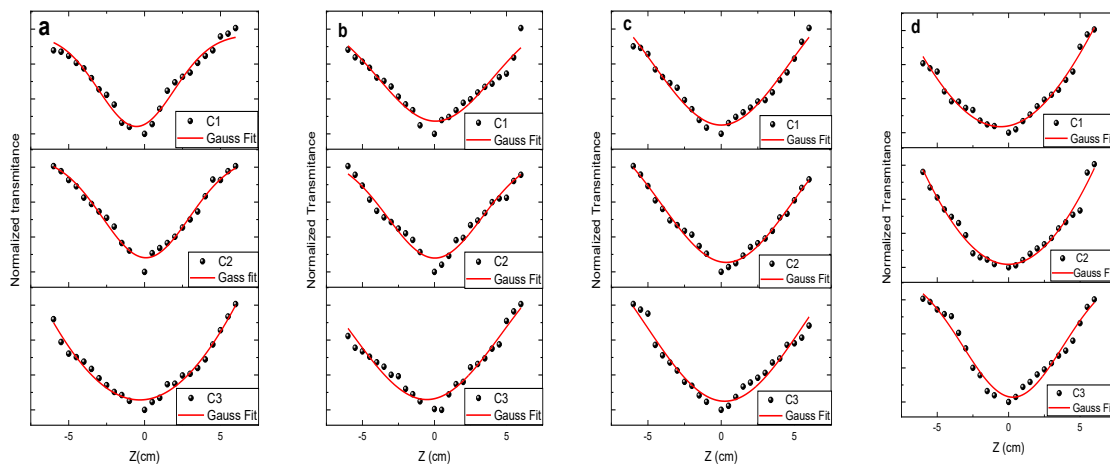


Fig. 9. Open aperture Z-Scan of a-c (532nm) and d for (635nm) a)100 mW, b)1000 mW, c)10000 Mw.

at a constant laser wavelength, varies from 0.5 cm/GW to 187 cm/GW, aligning with findings from previous research [18]. Notably, there is an increase in the difference in transmittance between peak and valley values that correlates directly with the emission power of the laser. This relationship suggests that higher laser powers enhance the material's nonlinear response. Fig. 10 visually represents this behavior by showing the exponential decay of the nonlinear absorption coefficient, plotted against the varying incident laser intensities [41]. This graph effectively illustrates how changes in laser intensity impact

the optical properties of the material, providing a clear understanding of the dynamic responses under different conditions.

To calculate the NLO refractive index n^2 , using close aperture Z-Scan method for three different concentration (C_1 , C_2 , C_3) 200 mW, 635nm. The transmittance peak to valley ΔT_{pv} given by the subsequent equation [42];

$$\Delta T_{pv} = 0.406 \Delta \phi \quad (5)$$

Where $\Delta \phi$ is non-linear phase shift and equal to $\Delta \phi = (2\pi/\lambda) n_2 L_{eff} I_0$. The measured value of

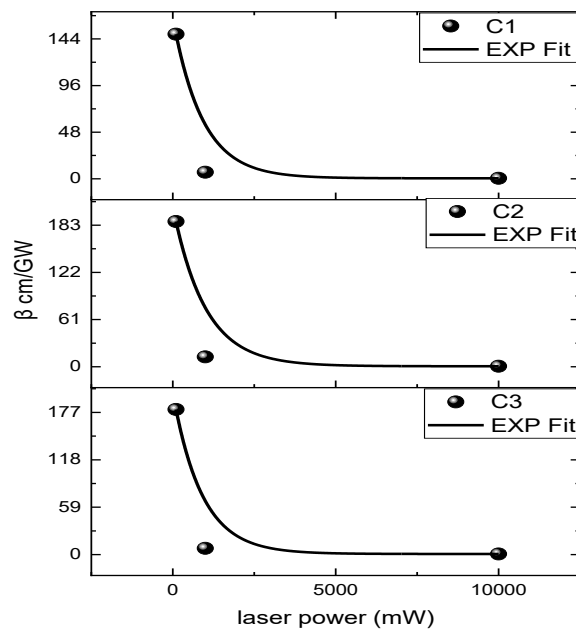


Fig. 10. Non-linear absorption coefficient β as a function of the incident laser power.

Table 3. z-scan data of ZnO Nano collide at different concentration.

Concentration /gm	Laser power /mW	λ /nm	β cm/GW
C1	100	532	148.95
	1000	532	6.765
	10000	532	0.506
	200	635	50.31
C2	100	532	187.80
	1000	532	12.76
	10000	532	0.657
	200	635	56.49
C3	100	532	180.70
	1000	532	7.7919
	10000	532	0.780
	200	635	68.886

non-linear refractive index is ranged between 2.51×10^{-13} and $5.81 \times 10^{-13} \text{ cm}^2/\text{W}$ are agreed with previous study [43, 44]. Focusing on the nonlinear optical (NLO) characteristics of ZnO nanoparticles, Fig. 11 illustrates the impact of nanoparticle colloid concentration on the single photon absorption coefficient and nonlinear refractive index, using a 200 mW excitation power

at a 635 nm wavelength. The data shows that both the nonlinear refractive index and nonlinear absorption coefficient decrease with the reduction in ZnO NP concentration. This trend suggests that smaller nanoparticle fractions, which occupy less volume, lead to reduced nonlinear optical coefficients. This relationship highlights that the NLO properties of nanoparticles are significantly

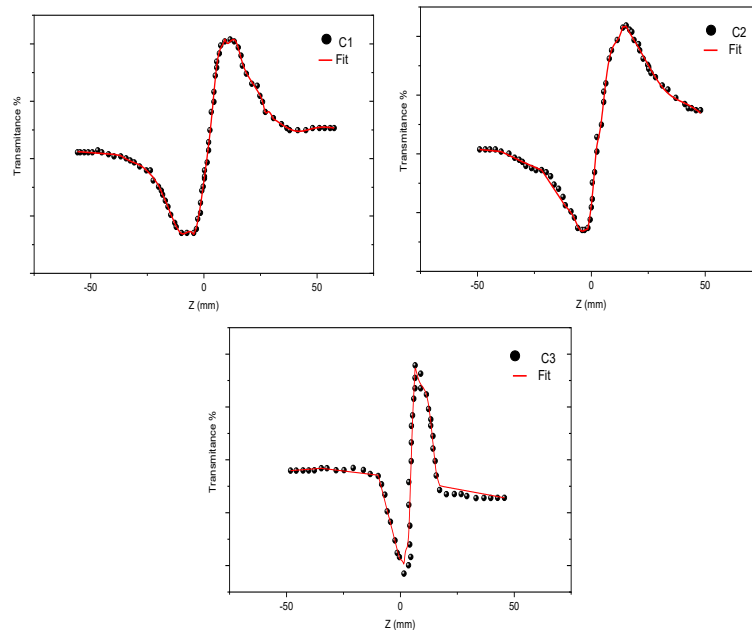


Fig. 11: Close aperture Z-Scan for 3 concentrations of ZnO NPs in distilled water using (200mW, 655nm).

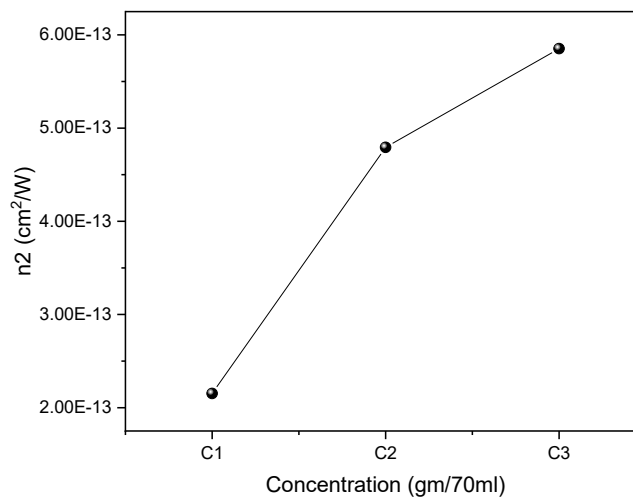


Fig. 12. Nonlinear refractive index (n^2) as a function of ZnO NP collide concentration.

influenced not only by their concentration but also by factors such as size, shape, and manufacturing process, along with the parameters of the excitation laser. These findings underscore the complex interdependencies that define the optical performance of nanoparticle-based systems.

Additionally, it is evident from the Z-scan trace that fluctuations in the concentration of ZnO nanoparticles lead to changes in the nonlinear phase shift, which in turn affects the nonlinear refractive index (n^2). As a result, as shown in Fig. 12, the magnitude of n^2 is dependent on the concentrations of ZnO nanoparticles in the nanocomposites [43]. This dependence highlights the sensitivity of the nonlinear optical properties to variations in nanoparticle concentration, underscoring the need for precise control over nanoparticle distribution within the composite to achieve desired optical characteristics.

CONCLUSION

This study has successfully demonstrated the synthesis of ZnO NPs using a green synthesis approach with mint plant extracts, tailored specifically for enhancing their efficacy in photonic applications. The characterization of these nanoparticles through SEM and XRD confirmed their nanoscale size and high crystallinity. Notably, the nanoparticles predominantly displayed a spherical and anisotropic morphology with an average size of about 80 nm, consistent with optimal properties for photonic device applications. The SEM and XRD analyses verified that the nanoparticles synthesized via this green method not only adhere to the desired physical attributes but also exhibit a significant improvement in structural and compositional integrity compared to nanoparticles synthesized through traditional methods. This enhancement is attributed to the effective roles of the phytochemicals present in the mint extract, which act as reducing, capping, and stabilizing agents, thus facilitating a more controlled and environmentally sustainable synthesis process. Further exploration of the nonlinear optical properties of these nanoparticles using both closed and open aperture Z-Scan techniques at varying laser powers and wavelengths demonstrated superior nonlinear absorption coefficients and refractive indices, marking a significant enhancement over the properties reported in previous studies. These findings not only underscore the potential of ZnO

NPs for advanced optical limiting applications but also highlight the advantages of integrating environmentally sustainable methods with nanoparticle technology, suggesting avenues for future research in refining synthesis processes and expanding applications into biomedical imaging and targeted drug delivery. This improvement in using ZnO nanoparticles shows how green synthesis methods can greatly benefit material science and photonic technologies, merging technological progress with environmental care.

ACKNOWLEDGEMENT

We would like to express our sincere gratitude to the Scientific Research Center of Soran University for their support and assistance throughout the course of this research project.

CONFLICT OF INTEREST

The authors declare that there is no conflict of interests regarding the publication of this manuscript.

REFERENCES

1. Gupta, S., J.F. Whitaker, and G.A. Mourou, Ultrafast carrier dynamics in III-V semiconductors grown by molecular-beam epitaxy at very low substrate temperatures. *IEEE Journal of Quantum Electronics*, 1992. 28(10): p. 2464-2472.
2. Kodikara, M.S., R. Stranger, and M.G. Humphrey, Computational studies of the nonlinear optical properties of organometallic complexes. *Coordination Chemistry Reviews*, 2018. 375: p. 389-409.
3. Non-Linear Optical Properties of Matter, in *Challenges and Advances in Computational Chemistry and Physics*. 2006, Springer Netherlands.
4. Fischer, P. and F. Hache, Nonlinear optical spectroscopy of chiral molecules. *Chirality*, 2005. 17(8): p. 421-437.
5. Zhuo, G.-Y., et al., Label-free multimodal nonlinear optical microscopy for biomedical applications. *Journal of Applied Physics*, 2021. 129(21).
6. Sankar, P. and R. Philip, Nonlinear Optical Properties of Nanomaterials, in *Characterization of Nanomaterials*. 2018, Elsevier. p. 301-334.
7. Chopra, K.L., S. Major, and D.K. Pandya, Transparent conductors—A status review. *Thin Solid Films*, 1983. 102(1): p. 1-46.
8. Jaffray, W., et al., Transparent conducting oxides: from all-dielectric plasmonics to a new paradigm in integrated photonics. *Advances in Optics and Photonics*, 2022. 14(2): p. 148.
9. Jiang, J., J. Pi, and J. Cai, The Advancing of Zinc Oxide Nanoparticles for Biomedical Applications. *Bioinorganic Chemistry and Applications*, 2018. 2018: p. 1-18.
10. Chen, D., et al., Preparation and photocatalytic properties of zinc oxide nanoparticles by microwave-assisted ball milling. *Ceramics International*, 2016. 42(2): p. 3692-3696.
11. Koao, L.F., F.B. Dejene, and H.C. Swart, Properties of flower-like ZnO nanostructures synthesized using the chemical

- bath deposition. *Materials Science in Semiconductor Processing*, 2014. 27: p. 33-40.
12. Darvishi, E., D. Kahrizi, and E. Arkan, Comparison of different properties of zinc oxide nanoparticles synthesized by the green (using *Juglans regia* L. leaf extract) and chemical methods. *Journal of Molecular Liquids*, 2019. 286: p. 110831.
13. Mirzaei, H. and M. Darroudi, Zinc oxide nanoparticles: Biological synthesis and biomedical applications. *Ceramics International*, 2017. 43(1): p. 907-914.
14. Singh, J., et al., 'Green' synthesis of metals and their oxide nanoparticles: applications for environmental remediation. *Journal of Nanobiotechnology*, 2018. 16(1).
15. Pantidos, N., Biological Synthesis of Metallic Nanoparticles by Bacteria, Fungi and Plants. *Journal of Nanomedicine and Nanotechnology*, 2014. 05(05).
16. Ovais, M., et al., Role of plant phytochemicals and microbial enzymes in biosynthesis of metallic nanoparticles. *Applied Microbiology and Biotechnology*, 2018. 102(16): p. 6799-6814.
17. Zinc Oxide — A Material for Micro- and Optoelectronic Applications, in *NATO Science Series II: Mathematics, Physics and Chemistry*. 2005, Springer Netherlands.
18. Sreeja, R., et al., Linear and nonlinear optical properties of luminescent ZnO nanoparticles embedded in PMMA matrix. *Optics Communications*, 2010. 283(14): p. 2908-2913.
19. Lin, J.-H., et al., Two-photon resonance assisted huge nonlinear refraction and absorption in ZnO thin films. *Journal of Applied Physics*, 2005. 97(3).
20. Özgür, Ü., et al., A comprehensive review of ZnO materials and devices. *Journal of Applied Physics*, 2005. 98(4).
21. Villeneuve, A., et al., Ultrafast all-optical switching in semiconductor nonlinear directional couplers at half the band gap. *Applied Physics Letters*, 1992. 61(2): p. 147-149.
22. Yang, C.C., et al., Effects of three-photon absorption on nonlinear directional coupling. *Optics Letters*, 1992. 17(10): p. 710.
23. Sheik-Bahae, M., et al., Sensitive measurement of optical nonlinearities using a single beam. *IEEE Journal of Quantum Electronics*, 1990. 26(4): p. 760-769.
24. Gómez, S.L., et al. Z-scan measurement of the nonlinear refractive indices of micellar lyotropic liquid crystals with and without the ferrofluid doping. *Physical Review E*, 1999. 59(3): p. 3059-3063.
25. Ramesh, M., M. Anbuvaran, and G. Viruthagiri, Green synthesis of ZnO nanoparticles using *Solanum nigrum* leaf extract and their antibacterial activity. *Spectrochimica Acta Part A: Molecular and Biomolecular Spectroscopy*, 2015. 136: p. 864-870.
26. Shnawa, B.H., et al., Scolicidal activity of biosynthesized zinc oxide nanoparticles by *Mentha longifolia* L. leaves against *Echinococcus granulosus* protoscolices. *Emergent Materials*, 2021. 5(3): p. 683-693.
27. Yedurkar, S., C. Maurya, and P. Mahanwar, Biosynthesis of Zinc Oxide Nanoparticles Using *Ixora coccinea* Leaf Extract—A Green Approach. *Open Journal of Synthesis Theory and Applications*, 2016. 05(01): p. 1-14.
28. Griffiths, P.R., *Fourier Transform Infrared Spectrometry*. Science, 1983. 222(4621): p. 297-302.
29. Al-Bayati, F.A., Isolation and identification of antimicrobial compound from *Mentha longifolia* L. leaves grown wild in Iraq. *Annals of Clinical Microbiology and Antimicrobials*, 2009. 8(1): p. 20.
30. Kamil, A.F., Green synthesis and eco- friendly methods to preparation of zinc oxide nanoparticles by extract of plants. *International Journal of Advanced Chemistry Research*, 2025. 7(4): p. 06-12.
31. Zandi, S., et al., Microstructure and optical properties of ZnO nanoparticles prepared by a simple method. *Physica B: Condensed Matter*, 2011. 406(17): p. 3215-3218.
32. Srivastava, V., D. Gusain, and Y.C. Sharma, Synthesis, characterization and application of zinc oxide nanoparticles (n-ZnO). *Ceramics International*, 2013. 39(8): p. 9803-9808.
33. Azad, A., et al., Factors Influencing the Green Synthesis of Metallic Nanoparticles Using Plant Extracts: A Comprehensive Review. *Pharmaceutical Fronts*, 2023. 05(03): p. e117-e131.
34. Alzahrani, E. and K. Welham, Optimization preparation of the biosynthesis of silver nanoparticles using watermelon and study of its antibacterial activity. *International Journal of Basic and Applied Sciences*, 2014. 3(4): p. 392.
35. Arumugam, M., et al., Green synthesis of zinc oxide nanoparticles (ZnO NPs) using *Syzygium cumini*: Potential multifaceted applications on antioxidants, cytotoxic and as nanonutrient for the growth of *Sesamum indicum*. *Environmental Technology & Innovation*, 2021. 23: p. 101653.
36. Barzinjy, A.A., et al., Biosynthesis, Characterization and Mechanism of Formation of ZnO Nanoparticles Using *Petroselinum crispum* Leaf Extract. *Current Organic Synthesis*, 2020. 17(7): p. 558-566.
37. Zhang, Y., et al., Hybrid Plasmonic Nanostructures with Unconventional Nonlinear Optical Properties. *Advanced Optical Materials*, 2014. 2(4): p. 331-337.
38. Mohamed, T., et al., Nonlinear Optical Properties of Zinc Oxide Nanoparticle Colloids Prepared by Pulsed Laser Ablation in Distilled Water. *Nanomaterials*, 2022. 12(23): p. 4220.
39. Saad, N.A., et al., Saturable and reverse saturable absorption of a Cu₂O-Ag nanoheterostructure. *Journal of Materials Science*, 2018. 54(1): p. 188-199.
40. Jamal, R.K., M.T. Hussein, and A.M. Suhail, Three-Photon Absorption in ZnO Film Using Ultra Short Pulse Laser. *Journal of Modern Physics*, 2012. 03(08): p. 856-864.
41. Díaz-Tovar, J.S., S. Valbuena-Duarte, and F. Racedo-Niebles, Study of non-linear optical properties in automobile lubricating oil via Z-Scan technique. *Revista Facultad de Ingeniería Universidad de Antioquia*, 2018(86): p. 27-31.
42. Liu, X., et al., Theoretical study on the closed-aperture Z-scan curves in the materials with nonlinear refraction and strong nonlinear absorption. *Optics Communications*, 2001. 197(4-6): p. 431-437.
43. Shanshool, H.M., et al., Third order nonlinearity of PMMA/ZnO nanocomposites as foils. *Optical and Quantum Electronics*, 2015. 48(1).
44. Rout, A., et al., Low- and high-order nonlinear optical studies of ZnO nanocrystals, nanoparticles, and nanorods. *The European Physical Journal D*, 2019. 73(11).